Compressibility of solid helium

Carlos P Herrero

Instituto de Ciencia de Materiales de Madrid, Consejo Superior de Investigaciones Científicas
(CSIC), Campus de Cantoblanco, 28049 Madrid, Spain

Abstract
The compressibility of solid helium (^{3}He and ^{4}He) in the hcp and fcc phases has been studied by
the path-integral Monte Carlo method. Simulations were carried out in both canonical (NVT)
and isothermal–isobaric (NPT) ensembles at temperatures between 10 and 300 K, showing
consistent results in both ensembles. For pressures between 4 and 10 GPa, the bulk modulus B
is found to decrease by about 10%, when the temperature increases from the low-temperature
limit to the melting temperature. The isotopic effect on the bulk modulus of helium crystals has
been quantified for a wide range of parameters. At 25 K and pressures on the order of 1 GPa,
the relative difference between ^{3}He and ^{4}He amounts to about 2%. The thermal expansion has
also been quantified from results obtained in both NPT and NVT simulations.

1. Introduction

In the last decades there has been continuous progress in the
study of different types of substances under extreme conditions
of pressure and temperature, thus enlarging appreciably the
experimentally accessible region of phase diagrams [1]. In
particular, the influence of controlled hydrostatic pressure on
the structural, thermodynamic, and electronic properties of
various kinds of solids has been intensively studied. Pressures
on the order of tens of GPa can now be routinely applied to real
materials [2–5].

Solid helium, in spite of having been studied for many
years, has a broad interest in condensed matter physics because
of its peculiar character as a 'quantum solid'. In particular,
its zero-point vibrational energy and associated anharmonic
effects are markedly larger than in most known solids [6].
In addition, its electronic simplicity allows one to carry out
detailed studies, that would be enormously difficult for other
materials [7–9]. The interest on the behaviour of solids under
high pressures has also been focused on solid helium. Thus,
diamond-anvil-cell and shock-wave experiments have allowed
the study of the equation of state (EOS) of solid ^{4}He up to
pressures on the order of 50 GPa [2, 10, 11]. In recent years,
the effect of pressure on heavier rare-gas solids has also been of
interest for both experimentalists [4, 12] and theorists [13–16].

The Feynman path-integral formulation of statistical me-
chanics [17, 18] is well suited to studying the thermodynamic
properties of solids at temperatures lower than their Debye
temperature Θ_D, where the quantum character of the atomic
nuclei becomes important. In particular, the combination
of path integrals with computer simulation methods, such as
Monte Carlo or molecular dynamics, has been revealed as a

powerful technique to carry out quantitative and nonperturba-
tive studies of many-body quantum systems at finite tempera-
tures. This has allowed the study of several properties of solids
further than the usual harmonic or quasiharmonic approxima-
tions [7].

The path-integral Monte Carlo (PIMC) method has been
used to study several properties of solid helium [7, 19–24],
as well as heavier rare-gas solids [25–30]. For helium, in
particular, this method has predicted kinetic-energy values [19]
and Debye–Waller factors [31] in good agreement with data
derived from experiments [32, 33]. PIMC simulations have
been also employed to study the isotopic shift in the helium
melting curve [20, 21]. The EOS of solid helium at $T = 0$
has been studied by diffusion Monte Carlo in a wide density
range [9, 34], as well as at finite temperatures by using PIMC
simulations with several interatomic potentials [22].

In recent years, there has been a debate on the existence of
supersolidity in ^{4}He at temperatures lower than 1 K [35–38].
This debate is still open, but is out of the scope of this paper,
since we consider here solid helium at temperatures higher than
10 K, where quantum exchange effects between atomic nuclei
are not relevant.

In this paper, we study the compressibility of solid ^{3}He and
^{4}He by PIMC simulations. We employ the isothermal–isobaric
(NPT) ensemble, which allows us to consider properties of
these solids along well-defined isobars. For comparison, we
also present results of PIMC simulations in the canonical
(NVT) ensemble. By comparing results for ^{3}He and ^{4}He, we
analyse isotopic effects on the compressibility as a function of
pressure.

The paper is organized as follows. In section 2, the
computational method is described. In section 3 we present

and discuss the results, divided into several subsections dealing with the thermodynamic consistency, pressure and temperature dependence of the bulk modulus, isotopic effects, and thermal expansion. Finally, in section 4 we present the conclusions.

2. Method

Equilibrium properties of solid ^{3}He and ^{4}He in the face-centred cubic (fcc) and hexagonal close-packed (hcp) phases have been calculated by PIMC simulations. The PIMC method relies on an isomorphism between the quantum system under consideration and a fictitious classical one, obtained by replacing each quantum particle by a cyclic chain of Q classical particles (Q: Trotter number), connected by harmonic springs with a temperature-dependent force constant. This isomorphism appears as a consequence of discretizing the density matrix along cyclic paths, which is usual in the path-integral formulation of statistical mechanics [17, 18]. Details of this computational method are given elsewhere [7, 39–41].

Helium atoms were considered as quantum particles interacting through an effective interatomic potential, composed of a two-body and a three-body part. For the two-body interaction, we employed the potential developed by Aziz *et al* [42] (the so-called HFD-B3-FCI1 potential). For the three-body part we took a Bruch–McGee-type potential [43, 44], with the parameters given by Loubeyre [44], but with parameter A in the attractive exchange interaction rescaled by a factor 2/3, as suggested in [21]. This interatomic potential was found earlier to describe well the vibrational energy and equation-of-state of solid helium over a broad range of pressures and temperatures [23].

Our simulations were based on the so-called 'primitive' form of PIMC [39, 45]. We considered two- and three-body terms explicitly in the simulations. The actual consideration of three-body terms did not allow us to use effective forms for the density matrix; these forms were developed to simplify the calculation when only two-body terms are explicitly considered [21]. Quantum exchange effects between atomic nuclei were not taken into account, because they are negligible for solid helium at the temperatures and pressures studied here. (This is expected to be valid assuming the absence of vacancies and for temperatures higher than the exchange frequency $\sim 10^{-6}$ K [7].) To calculate the energy we have used the 'crude' estimator, as defined in [39, 45].

We have employed both the canonical (NVT) ensemble and the isothermal–isobaric (NPT) ensemble. Our simulations were performed on supercells of the fcc and hcp unit cells, including 500 and 432 helium atoms respectively. To check the convergence of our results with system size, we carried out some simulations for other supercell sizes, and found that finite-size effects for $N > 400$ atoms are negligible for the quantities studied here. In particular, changes of the bulk modulus with the size of the simulation cell were found to be smaller than the statistical error bar of the values derived from our simulations.

Sampling of the configuration space was carried out by the Metropolis method at temperatures between 12 K and the melting temperature at each considered pressure. For given temperature and pressure, a typical run consisted of 10^4 Monte Carlo steps for system equilibration, followed by 4×10^5 steps for the calculation of ensemble average properties. Each step included attempts to move every replica of every atom in the simulation cell. In the NPT simulations, it also included an attempt to change the volume. To keep the accuracy of the computed quantities roughly constant at different temperatures, we took a Trotter number Q proportional to the inverse temperature, so that $QT = 3000$ K. This means that for solid helium at $T = 20$ K we had $Q = 150$, and a PIMC simulation for $N = 500$ atoms effectively includes 75000 'classical' particles. More technical details are given in [23, 29, 46].

In the NVT ensemble the pressure and isothermal bulk modulus $B = -V(\partial P/\partial V)_T$ can be obtained from thermal averages of various quantities obtained in PIMC simulations, as shown in appendix A. The derivation is straightforward from the partition function Z_{NVT} for N quantum particles in the canonical ensemble, but is rather tedious in the case of the bulk modulus, due to the number of terms appearing in the volume derivatives. In particular, B can be obtained from equations (A.11) and (A.12) in appendix A. In the NPT ensemble, the isothermal bulk modulus is related to the mean-square fluctuations of the volume V of the simulation cell by the expression:

$$\sigma_V^2 = \frac{V}{B} k_B T, \tag{1}$$

as shown in appendix B.

3. Results and discussion

3.1. Consistency checks

We have calculated the bulk modulus in the NPT and NVT ensembles. In general, we prefer the isothermal–isobaric ensemble, so that we can study solids along well-defined isotherms. NVT simulations are, however, frequently used in PIMC simulations [7, 19, 31], and a comparison of results obtained in both ensembles seems necessary as a consistency check of the method, and in particular for the case of solid helium.

We first discuss results obtained in the NPT ensemble. At constant pressure, the relative fluctuations in the volume, σ_V/V, can be found from equation (1):

$$\frac{\sigma_V}{V} = \left(\frac{k_B T}{BV} \right)^{\frac{1}{2}}. \tag{2}$$

For hcp ^{4}He at 25 K we found in PIMC simulations $\sigma_V/V = 2.9 \times 10^{-3}$ for $P = 2$ GPa, and a lower value of 1.4×10^{-3} for 20 GPa (for a simulation cell including $N = 432$ atoms). This means that the product BV increases as the pressure is raised (see equation (2)), in spite of the reduction of V, indicating that the growth of bulk modulus with pressure dominates in the product BV (see below).

For a cubic crystal, the fluctuations in the lattice parameter a can be derived from equation (1) to give:
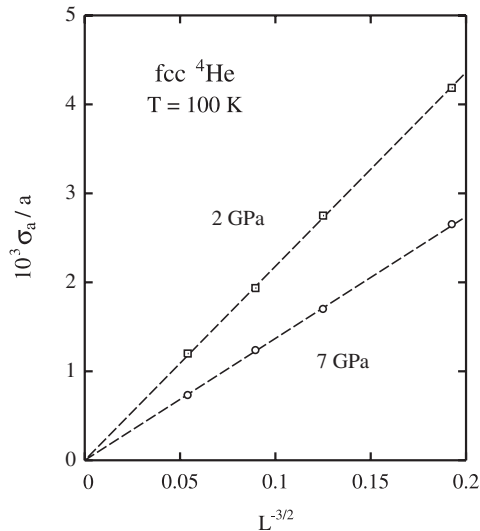
$$\sigma_a^2 = \frac{k_B T}{9 L^3 a B}, \tag{3}$$

Figure 1. Relative fluctuation of the lattice parameter, σ_a/a, of fcc ^{4}He versus $L^{-3/2}$, for simulation cells of lateral size La. Shown are results of PIMC simulations for two pressures (2 and 7 GPa) at $T = 100$ K, and for $L = 3, 4, 5$, and 7. Error bars are less than the symbol size.

Figure 2. Isothermal bulk modulus of solid ^{4}He as a function of pressure at three temperatures: 25 K (squares), 150 K (circles), and 300 K (triangles). Open and filled symbols correspond to hcp and fcc helium, respectively. Error bars are smaller than the symbol size. Dashed lines are fits to the data points using the expression: $B = B_0 + B_0'P + \frac{1}{2}B_0''P^2$.

where L^3 is the number of cubic unit cells in a simulation cell with side length La. From equation (3) one can see that the relative fluctuation in the lattice parameter, σ_a/a, scales as $L^{-3/2}$. This normalized fluctuation for fcc ^{4}He is displayed in figure 1 as a function of $L^{-3/2}$. Shown are results of PIMC simulations in the NPT ensemble at $T = 100$ K and two pressures: 2 and 7 GPa. The linear dependence shown in this figure agrees with the dependence of σ_a on the simulation-cell size given by equation (3). The different slopes of these lines are basically due to the change of compressibility with pressure.

To check the thermodynamic consistency of our simulations in both NPT and NVT ensembles we have carried out several tests. The first obvious test consists in taking the crystal volume derived from isothermal–isobaric simulations, and using it as an input in NVT simulations at the same temperature. The latter should give the same pressure (using equation (A.7)) as that used earlier in the NPT simulations. As an example, for fcc ^{4}He at 25 K and 1 GPa, we find first a lattice parameter $a = 3.6955$ Å, that introduced as an input in NVT simulations yields a pressure of 1.0002(5) GPa, in good agreement with the input in the previous NPT simulations. Going on with the same set of parameters, we can also check the consistency of the bulk modulus B derived from both types of simulations. At constant pressure ($P = 1$ GPa), we find $B_{NPT} = 4.50(2)$ GPa from the volume fluctuations (see equation (B.5) in appendix B) versus $B_{NVT} = 4.47(2)$ GPa derived at constant volume by using expressions (A.11) and (A.12).

3.2. Pressure and temperature dependence

We now consider the pressure dependence of the bulk modulus, as derived from our PIMC simulations. This is shown in figure 2 for ^{4}He at three temperatures. In this figure, T
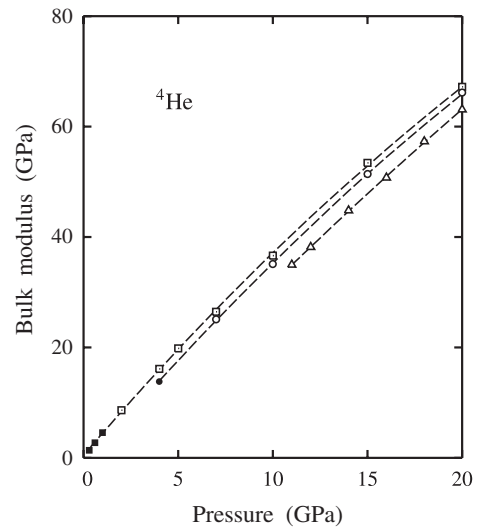
decreases from top to bottom: $T = 25, 150$, and 300 K; open and filled symbols correspond to hcp and fcc helium, respectively. At each considered temperature, we present data for the pressure region where the solid was stable (or metastable) along the PIMC simulations, a region that becomes broader as the temperature is lowered. In addition to the typical rise of B for increasing pressure, we find that for a given pressure, B decreases as the temperature is raised. In the pressure range shown in figure 2 one also observes a departure from linearity in the dependence of B on pressure. By fitting these results to the expression $B = B_0 + B_0'P + \frac{1}{2}B_0''P^2$, we can find the pressure derivatives at $P = 0$ (B_0' and B_0''). Thus, for $T = 25$ K we obtain $B_0 = 0.47$ GPa, $B_0' = 4.01$, and $B_0'' = -0.068$ GPa^{-1}.

For the other temperatures shown in figure 2 ($T = 150$ and 300 K), an extrapolation of the results to $P = 0$ yields negative values of B_0, indicating that the solid is mechanically unstable at these temperatures for low pressures. At 25 K and zero pressure, even though the liquid is known to be the stable phase, the solid can still be metastable, as it has not yet reached the limit of mechanical stability, or the spinodal line. Apart from this, the curves $B(P)$ at the considered temperatures are rather parallel one to the other in the common stability region.

It is interesting to compare the bulk modulus obtained here for solid helium with those of heavier rare-gas solids at the same conditions. For example, at $T = 20$ K and $P = 1$ GPa, we find for solid ^{4}He: $B = 4.53$ GPa, versus 7.20 and 9.43 for Ne and Ar, respectively [30]. This is in line with the known result that the bulk modulus increases with atomic mass for given values of temperature and pressure [30].

Rare-gas solids have been studied in metastable conditions, even at negative pressures [47]. They have been found to be metastable in PIMC simulations close to the spinodal point, defined as the point at which the compressibility $\kappa = 1/B$
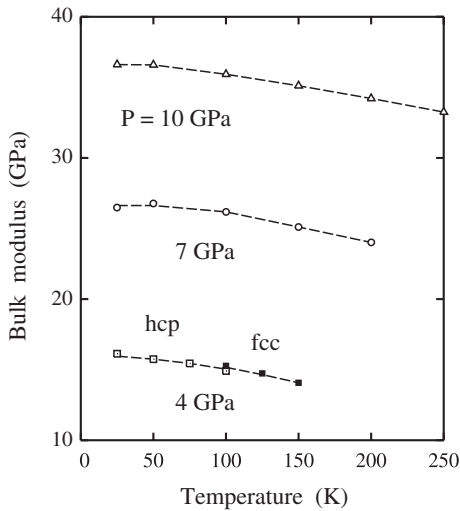
Figure 3. Isothermal bulk modulus of solid ^{4}He as a function of temperature at three hydrostatic pressures: 4 GPa (squares), 7 GPa (circles), and 10 GPa (triangles). Open and filled symbols correspond to hcp and fcc helium, respectively. Error bars of the simulation results are on the order of the symbol size. Dashed lines are guides to the eye.

Figure 4. Isothermal bulk modulus of solid ^{4}He versus density. Open squares represent results of path-integral Monte Carlo simulations in the NPT ensemble. Error bars are less than the symbol size. A solid line indicates the bulk modulus derived by Zha *et al* [48] from Brillouin scattering experiments. The dashed line is a guide to the eye.

diverges (or the bulk modulus vanishes). Thus, for solid Ne and Ar at 5 K, the spinodal point was found at $P = -91$ and -245 MPa. For solid helium, we could not approach the spinodal point at any temperature, due to the large quantum fluctuations that make the solid unstable along the simulations. This happened even at zero pressure and relatively low temperature, in spite of the fact that the expected bulk modulus at these conditions is still far from vanishing. For example, at 25 K we find for solid helium $B_0 = 0.47$ GPa, as derived from extrapolation of the results obtained at $P > 0.2$ GPa (see above and figure 2), but the solid was unstable in our simulations at $P < 0.2$ GPa.

The temperature dependence of the bulk modulus is displayed in figure 3 for three different pressures. Here again open and filled symbols indicate hcp and fcc helium, respectively. For each pressure under consideration, the plotted data correspond to the temperature region where we found the solids to be (meta)stable along the PIMC simulations. For each pressure, the bulk modulus decreases as the temperature is raised, and this decrease is similar for different pressures. In fact, the obtained curves $B(T)$ are parallel within the statistical error of our simulations. In the whole accessible temperature range, the bulk modulus decreases by 2.1, 2.6, and 3.1 GPa, for $P = 4$, 7, and 10 GPa, respectively. These values amount to 13.0, 9.8, and 8.5% of the corresponding bulk modulus at 25 K.

To connect with data derived from experiment, we note that Zha *et al* [48] have obtained the bulk modulus of solid ^{4}He from Brillouin scattering measurements. From these results, they derived the dependence of the isothermal bulk modulus upon material density at 300 K. In figure 4 we present results of our PIMC simulations for ^{4}He at 300 K (open squares) along with those derived from Brillouin scattering experiments at room temperature (solid line). At this temperature, the density region between 0.95 and 1.25 g cm^{-3} corresponds to a pressure between 12 and 29 GPa. At $\rho < 1$ g cm^{-3}, our results coincide
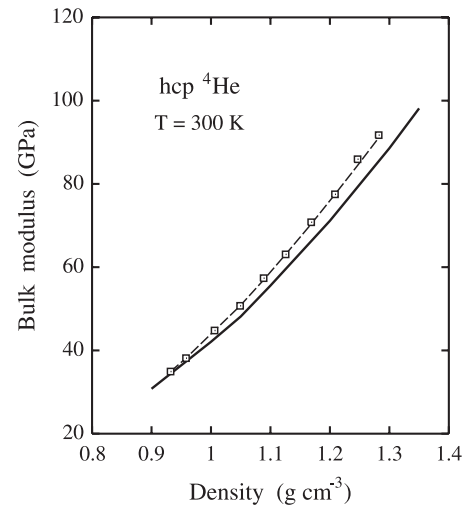
within error bars with those derived from Brillouin scattering, and at higher densities the bulk modulus derived from PIMC simulations is somewhat larger. For example, at density $\rho = 1$ and 1.25 g cm^{-3}, Zha *et al* [48] obtained $B = 42.1$ and 79.9 GPa respectively, to be compared with $B = 44$ and 86 GPa yielded by our PIMC simulations of ^{4}He at the same densities and $T = 300$ K. This means that at $\rho = 1.25$ g cm^{-3}, the difference amounts to about 7%.

3.3. Isotopic effect

An interesting point in this context is the influence of the atomic mass on the solid compressibility. This isotopic effect can be readily obtained from PIMC simulations, since the mass is an input parameter in these calculations. Similar isotopic effects have been studied earlier for the melting curve [20, 21] and molar volume [23, 24] of solid helium. For a given material, lighter isotopes form more compressible solids, as a consequence of an increase in the molar volume. This is in fact due to a combination of the anharmonicity in the interatomic potential and zero-point vibrations, which are most important at low temperature. Since these quantum vibrations are especially large in the case of helium, due to its low mass, the isotopic effect on the bulk modulus is expected to be appreciable.

Thus, one expects the bulk modulus of solid ^{4}He to be larger than that of ^{3}He. This is in fact the case, as derived from our PIMC simulations. In figure 5 we display the difference $\Delta B = B_4 - B_3$ as a function of pressure at $T = 25$ K. For example, at 1 GPa and 25 K we find $B = 4.40$ and 4.50 ± 0.01 GPa for ^{3}He and ^{4}He, respectively, and the difference between both isotopes amounts to 2.2%. At the same temperature and 7 GPa, we obtained $B = 26.20$ and 26.59 GPa, which translates to a relative difference of 1.5%. This relative change in bulk modulus associated to the isotopic
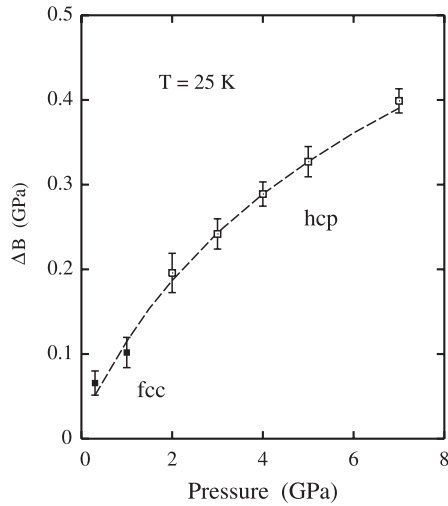
Figure 5. Isotopic effect on the isothermal bulk modulus as a function of pressure. Shown is the difference $\Delta B = B_4 - B_3$ between the bulk modulus of ^{4}He and ^{3}He at 25 K. Filled and open symbols represent data for fcc and hcp helium, respectively.
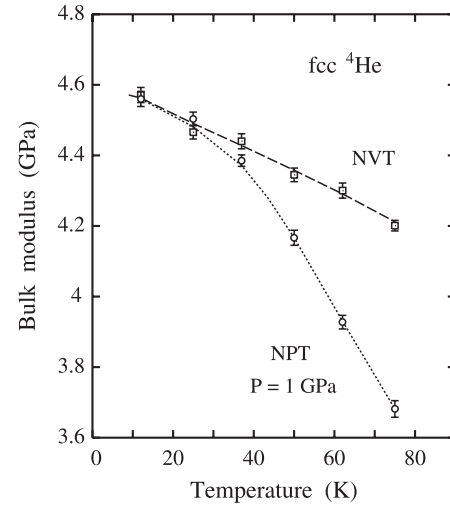

Figure 6. Bulk modulus versus temperature, as derived from PIMC simulations at constant volume (squares) and constant pressure (circles). The simulations in the NVT ensemble were carried out with the volume obtained at $P = 1$ GPa and $T = 25$ K. Lines are guides to the eye.

mass is appreciable, and slightly larger than that found for the isotopic effect on the molar volume of helium crystals. Thus, at a pressure of 1 and 7 GPa and $T = 25$ K, we find a volume difference of 1.8 and 0.9%, when comparing ^{3}He and ^{4}He [24]. In general, given a temperature, the relative changes in volume and compressibility decrease for increasing pressure, since the solid behaves as if it was 'more classical' [30, 49], and isotopic effects (of quantum origin) are consequently reduced.

3.4. Thermal expansion

At this point, it is worthwhile comparing the temperature dependence of the bulk modulus obtained at fixed volume and fixed pressure, from PIMC simulations in the NVT and NPT ensembles, respectively. In figure 6 we have plotted our results for B, as derived in both cases. On one side, the simulations in the isothermal–isobaric ensemble were carried out at a pressure $P = 1$ GPa, and the results obtained are represented in figure 6 as circles. On the other side, simulations in the canonical ensemble (at various temperatures) were performed for the volume obtained in NPT simulations at $T = 25$ K and $P = 1$ GPa. Results of these NVT simulations are displayed as open squares. As expected, B obtained in both types of simulations agree with each other (within error bars) at $T \leqslant 25$ K. At higher temperatures, the NPT simulations yield values of the bulk modulus smaller than those derived from NVT simulations. This is due to the thermal expansion, that is taken into account in the simulations at constant pressure, but is neglected in the constant-volume simulations. In general, an increase in crystal volume causes a decrease in the bulk modulus.

In this context, another application of our PIMC simulations consists in the calculation of the thermal expansion coefficient

$$\alpha = \frac{1}{V} \left(\frac{\partial V}{\partial T} \right)_P, \tag{4}$$

which can be obtained in the canonical ensemble by using the expression [50]:

$$\alpha = \frac{1}{B} \left(\frac{\partial P}{\partial T} \right)_V. \tag{5}$$

This equation in fact relates the thermal expansion with the compressibility through the temperature derivative of the pressure at constant volume. In connection with equation (5), we note that the pressure obtained in NVT simulations (with a fixed lattice parameter $a = 3.6955$ Å) increases from 1 to 1.3 GPa when the temperature rises from 25 to 75 K. At 25 K, we have $B = 4.46$ GPa and $(\partial P/\partial T)_V = 8.87 \times 10^{-4}$ GPa K^{-1}, giving $\alpha_{NVT} = 1.99 \times 10^{-4}$ K^{-1}. This result is in agreement with that found directly from the volume change obtained in the NPT simulations, which yields $\alpha_{NPT} = 2.03 \times 10^{-4}$ K^{-1}.

Finally, in figure 7 we present results of the thermal expansion coefficient α yielded by our simulations in the isothermal–isobaric ensemble at two (high) pressures. We give values for both ^{3}He and ^{4}He in the hcp phase. First, we observe an important decrease in α as the pressure is raised. For ^{4}He at 300 K, we find a reduction in α by a factor of five, when increasing P from 12 to 52 GPa. Second, we note that the thermal expansion is smaller for ^{3}He than for ^{4}He. This is easy to understand, since the molar volume of solid ^{3}He is larger than that of ^{4}He [23], and both volumes have to converge one to the other in the high-temperature (classical) limit.

4. Conclusions

Path-integral Monte Carlo simulations in both NVT and NPT ensembles have been shown to be well suited to analyse the temperature and pressure dependence of the bulk modulus of solid helium. In the isothermal–isobaric ensemble, B can be derived from the volume fluctuations along a simulation run. In the canonical ensemble, a calculation of B is more
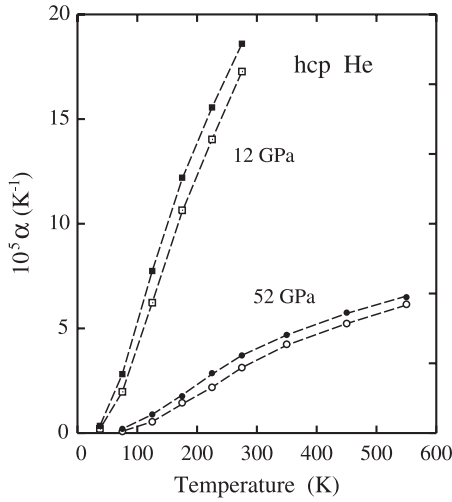
Figure 7. Temperature dependence of the thermal expansion coefficient α of hcp helium, as derived from PIMC simulations at $P = 12$ and 52 GPa. Open and filled symbols correspond to ^{3}He and ^{4}He, respectively. Error bars are on the order of the symbol size. Dashed lines are guides to the eye.

elaborate, but can be carried out from thermal averages of various intermediate quantities obtained in PIMC simulations. Both ensembles NVT and NPT give consistent results for the compressibility and thermal expansion of ^{3}He and ^{4}He in the whole region of temperatures and pressures considered here.

At a given pressure, the bulk modulus decreases as temperature rises. For pressures between 4 and 10 GPa, the change in B has been found to be on the order of 10%, when temperature increases from the low-T limit to the melting temperature of the material.

Solid ^{3}He is more compressible than ^{4}He. At a given T, the difference between the bulk modulus of both solids increases as pressure rises, but the relative difference between them decreases. This isotopic effect on the compressibility of solid helium is appreciable in the range of temperatures and pressures studied here. In fact, at 25 K and pressures on the order of 1 GPa, it amounts to about 2%.

Apart from a precise calculation of the bulk modulus, PIMC simulations in the canonical ensemble can be also used to study accurately the thermal expansion of the solids under consideration at a given pressure.

Acknowledgments

Appendix A. Pressure and bulk modulus in the NVT ensemble

A.1. Pressure

In the path-integral formalism, the canonical partition function for N identical quantum particles obeying Boltzmann statistics (no particle exchange) can be written as [39, 40]:

$$Z_{NVT} = K \int \prod_{i=1}^{N} \prod_{j=1}^{Q} d\mathbf{r}_{ij} \exp\left(-\beta \sum_{j=1}^{Q}\left[C \sum_{i=1}^{N}(\mathbf{r}_{i,j+1} - \mathbf{r}_{ij})^2 \right.\right.$$
$$\left.\left. + \frac{1}{Q}\, \Phi(\mathbf{r}_{1j}, \ldots, \mathbf{r}_{Nj})\right]\right), \quad\quad\text{(A.1)}$$

where $\mathbf{r}_{ij}$ ($i = 1, \ldots, N$; $j = 1, \ldots, Q$) are Cartesian coordinates of the N particles at imaginary time j, $\beta = (k_B T)^{-1}$, and $\Phi(\mathbf{r}_{1j}, \ldots, \mathbf{r}_{Nj})$ is the potential energy. We have defined

$$K = \frac{1}{N!}\left(\frac{mQ}{2\pi\beta\hbar^2}\right)^{3NQ/2} \quad\quad\text{(A.2)}$$

and

$$C = \frac{mQ}{2\beta^2\hbar^2}. \quad\quad\text{(A.3)}$$

The coordinates are subject to the cyclic condition $\mathbf{r}_{i,Q+1} = \mathbf{r}_{i1}$ for all particles $i = 1, \ldots, N$. Changing $\mathbf{r}_{ij}$ to reduced coordinates $\mathbf{s}_{ij} = V^{-1/3}\mathbf{r}_{ij}$, we find:

$$Z_{NVT} = KV^{NQ} \int \prod_{i=1}^{N} \prod_{j=1}^{Q} d\mathbf{s}_{ij} \exp\left[-\beta H(\beta, V, \{\mathbf{s}_{ij}\})\right], \quad\quad\text{(A.4)}$$

where we have defined

$$H(\beta, V, \{\mathbf{s}_{ij}\}) = CV^{2/3} \sum_{i=1}^{N} \sum_{j=1}^{Q}(\mathbf{s}_{i,j+1} - \mathbf{s}_{ij})^2$$
$$+ \frac{1}{Q} \sum_{j=1}^{Q} \Phi(V^{1/3}\mathbf{s}_{1j}, \ldots, V^{1/3}\mathbf{s}_{Nj}) \quad\quad\text{(A.5)}$$

and the dependence of H on β, V, and the coordinates $\mathbf{s}_{ij}$ has been explicitly indicated.

The pressure is given by

$$P = \frac{1}{\beta} \frac{1}{Z_{NVT}} \frac{\partial Z_{NVT}}{\partial V}, \quad\quad\text{(A.6)}$$

and from the volume derivative of Z_{NVT} one finds:

$$P = \frac{NQ}{\beta V} - \frac{2}{3V}\langle E_h \rangle - \langle \Phi_V \rangle \quad\quad\text{(A.7)}$$

where E_h refers to the 'harmonic' energy:

$$E_h = C \sum_{i=1}^{N} \sum_{j=1}^{Q}(\mathbf{r}_{i,j+1} - \mathbf{r}_{ij})^2 = CV^{2/3} \sum_{i=1}^{N} \sum_{j=1}^{Q}(\mathbf{s}_{i,j+1} - \mathbf{s}_{ij})^2 \quad\quad\text{(A.8)}$$

and

$$\Phi_V = \frac{1}{Q} \sum_{j=1}^{Q} \frac{\partial \Phi(V^{1/3}\mathbf{s}_{1j}, \ldots, V^{1/3}\mathbf{s}_{Nj})}{\partial V}. \quad\quad\text{(A.9)}$$

A.2. Bulk modulus

The isothermal bulk modulus is:

$$B = -V\left(\frac{\partial P}{\partial V}\right)_T \quad\quad\text{(A.10)}$$

and substituting equation (A.6) for the pressure, we have:

$$B = V\beta P^2 - \frac{V}{\beta Z_{NVT}} \frac{\partial^2 Z_{NVT}}{\partial V^2}. \quad (A.11)$$

Taking a second volume derivative of Z_{NVT}, we find:

$$\frac{1}{\beta Z_{NVT}} \frac{\partial^2 Z_{NVT}}{\partial V^2} = \frac{NQ(NQ-1)}{\beta V^2}$$
$$+ \frac{1}{3V^2}\left(\frac{2}{3} - 4NQ\right)\langle E_{\mathrm{h}}\rangle - \frac{2NQ}{V}\langle \Phi_V\rangle + \frac{4}{9}\frac{\beta}{V^2}\langle E_{\mathrm{h}}^2\rangle$$
$$+ \frac{4}{3}\frac{\beta}{V}\langle E_{\mathrm{h}}\Phi_V\rangle - \frac{1}{Q}\left\langle\frac{\partial\Phi_V}{\partial V}\right\rangle + \beta\langle\Phi_V^2\rangle. \quad (A.12)$$

Finally, equations (A.11) and (A.12) give us the bulk modulus B at volume V and temperature T.

Appendix B. Compressibility in the NPT ensemble

We now have the partition function

$$Z_{NPT} = \int_0^\infty \mathrm{d}V\, \mathrm{e}^{-\beta PV} Z_{NVT}. \quad (B.1)$$

To obtain the compressibility, we calculate the pressure derivatives of $\ln Z_{NPT}$. We find:

$$\frac{\partial \ln Z_{NPT}}{\partial P} = \frac{1}{Z_{NPT}}\frac{\partial Z_{NPT}}{\partial P} = -\beta\langle V\rangle \quad (B.2)$$

and

$$\frac{\partial^2 \ln Z_{NPT}}{\partial P^2} = -\frac{1}{Z_{NPT}^2}\left(\frac{\partial Z_{NPT}}{\partial P}\right)^2 + \frac{1}{Z_{NPT}}\frac{\partial^2 Z_{NPT}}{\partial P^2}$$
$$= -\beta^2\langle V\rangle^2 + \beta^2\langle V^2\rangle = -\beta^2\sigma_V^2, \quad (B.3)$$

where σ_V^2 is the mean-square fluctuation of the volume. Moreover, from equation (B.2):

$$\frac{\partial^2 \ln Z_{NPT}}{\partial P^2} = -\beta\frac{\partial\langle V\rangle}{\partial P}, \quad (B.4)$$

and from equations (B.3) and (B.4), we obtain for the isothermal compressibility κ:

$$\kappa = -\frac{1}{\langle V\rangle}\left(\frac{\partial\langle V\rangle}{\partial P}\right)_T = \frac{\beta\sigma_V^2}{\langle V\rangle}. \quad (B.5)$$

This is the thermodynamic relation obtained in general in the isothermal–isobaric ensemble [51]. Thus, it can be directly used to obtain the compressibility from the volume fluctuations in path-integral simulations, without any further calculations.

References

[1] Young D A 1991 *Phase Diagrams of the Elements* (Berkeley, CA: University of California Press)
[2] Loubeyre P, LeToullec R, Pinceaux J P, Mao H K, Hu J and Hemley R J 1993 *Phys. Rev. Lett.* **71** 2272
[3] Hemley R J, Zha C S, Jephcoat A P, Mao H K, Finger L W and Cox D E 1989 *Phys. Rev. B* **39** 11820
[4] Shimizu H, Tashiro H, Kume T and Sasaki S 2001 *Phys. Rev. Lett.* **86** 4568
[5] Errandonea D, Boehler R, Japel S, Mezouar M and Benedetti L R 2006 *Phys. Rev. B* **73** 092106
[6] Glyde H R 1976 *Rare Gas Solids* ed M L Klein and J A Venables (New York: Academic) pp 382–504
[7] Ceperley D M 1995 *Rev. Mod. Phys.* **67** 279
[8] Nabi Z, Vitos L, Johansson B and Ahuja R 2005 *Phys. Rev. B* **72** 172102
[9] Cazorla C and Boronat J 2008 *J. Phys.: Condens. Matter* **20** 015223
[10] Polian A and Grimsditch M 1986 *Europhys. Lett.* **2** 849
[11] Mao H K, Hemley R J, Wu Y, Jephcoat A P, Finger L W, Zha C S and Bassett W A 1988 *Phys. Rev. Lett.* **60** 2649
[12] Errandonea D, Schwager B, Boehler R and Ross M 2002 *Phys. Rev. B* **65** 214110
[13] Neumann M and Zoppi M 2000 *Phys. Rev. B* **62** 41
[14] Iitaka T and Ebisuzaki T 2001 *Phys. Rev. B* **65** 012103
[15] Dewhurst J K, Ahuja R, Li S and Johansson B 2002 *Phys. Rev. Lett.* **88** 075504
[16] Tsuchiya T and Kawamura K 2002 *J. Chem. Phys.* **117** 5859
[17] Feynman R P 1972 *Statistical Mechanics* (New York: Addison-Wesley)
[18] Kleinert H 1990 *Path Integrals in Quantum Mechanics, Statistics and Polymer Physics* (Singapore: World Scientific)
[19] Ceperley D M, Simmons R O and Blasdell R C 1996 *Phys. Rev. Lett.* **77** 115
[20] Barrat J L, Loubeyre P and Klein M L 1989 *J. Chem. Phys.* **90** 5644
[21] Boninsegni M, Pierleoni C and Ceperley D M 1994 *Phys. Rev. Lett.* **72** 1854
[22] Chang S Y and Boninsegni M 2001 *J. Chem. Phys.* **115** 2629
[23] Herrero C P 2006 *J. Phys.: Condens. Matter* **18** 3469
[24] Herrero C P 2007 *J. Phys.: Condens. Matter* **19** 156208
[25] Cuccoli A, Macchi A, Tognetti V and Vaia R 1993 *Phys. Rev. B* **47** 14923
[26] Müser M H, Nielaba P and Binder K 1995 *Phys. Rev. B* **51** 2723
[27] Chakravarty C 2002 *J. Chem. Phys.* **116** 8938
[28] Neumann M and Zoppi M 2002 *Phys. Rev. E* **65** 031203
[29] Herrero C P 2002 *Phys. Rev. B* **65** 014112
[30] Herrero C P and Ramírez R 2005 *Phys. Rev. B* **71** 174111
[31] Draeger E W and Ceperley D M 2000 *Phys. Rev. B* **61** 12094
[32] Arms D A, Shah R S and Simmons R O 2003 *Phys. Rev. B* **67** 094303
[33] Venkataraman C T and Simmons R O 2003 *Phys. Rev. B* **68** 224303
[34] Moroni S, Pederiva F, Fantoni S and Boninsegni M 2000 *Phys. Rev. Lett.* **84** 2650
[35] Kim E and Chan M H W 2004 *Nature* **427** 225
[36] Rittner A S C and Reppy J D 2007 *Phys. Rev. Lett.* **98** 175302
[37] Clark A C, West J T and Chan M H W 2007 *Phys. Rev. Lett.* **99** 135302
[38] Ceperley D M and Bernu B 2004 *Phys. Rev. Lett.* **93** 155303
[39] Chandler D and Wolynes P G 1981 *J. Chem. Phys.* **74** 4078
[40] Gillan M J 1988 *Phil. Mag.* A **58** 257
[41] Noya J C, Herrero C P and Ramírez R 1996 *Phys. Rev. B* **53** 9869
[42] Aziz R A, Janzen A R and Moldover M R 1995 *Phys. Rev. Lett.* **74** 1586
[43] Bruch L W and McGee I J 1973 *J. Chem. Phys.* **59** 409
[44] Loubeyre P 1987 *Phys. Rev. Lett.* **58** 1857
[45] Singer K and Smith W 1988 *Mol. Phys.* **64** 1215
[46] Noya J C, Herrero C P and Ramírez R 1997 *Phys. Rev. B* **56** 237
[47] Herrero C P 2003 *Phys. Rev. B* **68** 172104
[48] Zha C S, Mao H K and Hemley R J 2004 *Phys. Rev. B* **70** 174107
[49] Etters R D and Danilowicz R L 1974 *Phys. Rev. A* **9** 1698
[50] Callen H B 1960 *Thermodynamics* (New York: Wiley)
[51] Landau L D and Lifshitz E M 1980 *Statistical Physics* 3rd edn (Oxford: Pergamon)